(This is a sample cover image for this issue. The actual cover is not yet available at this time.)

Earth and Planetary Science Letters 310 (2011) 314–318

Contents lists available at SciVerse ScienceDirect

Earth and Planetary Science Letters

journal homepage: www.elsevier.com/locate/epsl

Jarosite, argon diffusion, and dating aqueous mineralization on Earth and Mars

Joseph Kula *, Suzanne L. Baldwin

Department of Earth Sciences, Syracuse University, Syracuse, NY 13244, United States

ARTICLE INFO

Article history:
Received 8 June 2011
Received in revised form 20 July 2011
Accepted 8 August 2011
Available online xxxx

Edited by R.W. Carlson

Keywords:
jarosite
argon diffusion
Mars
thermochronology
dating aqueous environments

ABSTRACT

Jarosite $^{40}Ar/^{39}Ar$ ages can be used to date surface processes such as weathering and environmental transitions (i.e. aridification) on Earth and Mars. To better interpret jarosite ages from a thermochronological perspective, the diffusion kinetics of argon in jarosite were determined. Incremental fractional loss measurements indicate an activation energy (E) of 37.8 ± 1.5 kcal/mol and a log D_o/a^2 of 5.68 ± 0.63 s^{-1} corresponding to a closure temperature of 143 ± 28 °C, assuming a cooling rate 100 °C/Ma. Downward extrapolation of these parameters to Martian surface temperatures (≤22 °C) predicts <1% fractional loss of Ar over 4.0 Ga. Forward modeling of $^{40}Ar/^{39}Ar$ age spectra using the least retentive E, D_o/a^2 pairs predict that if held at 22 °C or less for 4.0 Ga, supergene jarosite would preserve original growth ages manifest as plateau ages consisting of >95% of the gas release. Because of its susceptibility to mineralogical breakdown, $^{40}Ar/^{39}Ar$ ages on preserved Martian jarosite will reflect the time since water was present at a location that has since undergone aridification and remained hydrologically inactive and thermally quiescent.

1. Introduction

The landing site at Meridiani Planum for the Mars exploration rover (MER) *Opportunity* was selected based in part on remote sensing data from orbiters that indicated the presence of hematite hypothesized to be the product of aqueous weathering processes (Christensen et al., 2000). Using the Mossbauer spectrometer aboard *Opportunity*, the hydrous, potassium-bearing iron sulfate, jarosite [$K_2Fe_3(SO_4)_2(OH)_6$], was detected in Martian sediments at Eagle Crater (Klingelhofer, 2004) and subsequently found throughout the deposits at Meridiani Planum (Squyres and Knoll, 2005). The presence of jarosite on Mars has two first-order astrobiological implications: 1) as an (OH)-bearing mineral, jarosite requires the presence of water during its formation, and 2) as a K-bearing mineral, jarosite has been demonstrated as a reliable terrestrial chronometer using the $^{40}Ar/^{39}Ar$ method (Lueth et al., 2005; Vasconcelos et al., 1994). When these two implications are combined, it is evident that measuring an isotopic age on jarosite may not only record the time since formation of the mineral, but also the time since water was present at that location. This paired significance provides a basis for continued study of jarosite and is consistent with the fundamental principle of "follow the water" that has guided the ongoing search for evidence of life on Mars. Additionally, because jarosite is present on Earth, it can be studied at length in the context of its Martian occurrence (as constrained by orbiters and MERs) prior to being retrieved during Mars sample return missions (Burger et al., 2009; Madden et al., 2004; Papike et al., 2006).

With the recent transition in Mars exploration program themes from "follow the water" to "explore habitable environments", jarosite remains on the list of key astrobiologically significant subjects for continued research. Evaporitic sulfate minerals have been shown to preserve amino acids and amines over geologically long time periods on Earth (Aubrey et al., 2006), and glycine has been recovered from natural jarosite samples (Kotler et al., 2008). Therefore, just as the hydrous chemistry of jarosite rendered it significant towards identifying aqueous environments, its sulfate character implicates jarosite as a potential preserver of biological signatures. Jarosite-bearing locations have been recommended as targets for future sample return missions to Mars (Navrotsky et al., 2005; Papike et al., 2006) at least in part because of these characteristics. To date, however, it remains unknown the degree to which Martian jarosite may, or may not, retain original argon isotopic signatures recording the timing of formation and, by extension, the age of transient jarosite-forming aqueous conditions.

To better interpret measured $^{40}Ar/^{39}Ar$ ages within their petrologic context, the kinetics of argon diffusion in jarosite were determined. Results are used to evaluate the argon retention behavior of jarosite as it relates to the processes by which this mineral forms on Earth. Fractional loss calculations and model constraints on the long-term retention of argon in jarosite are discussed from a thermochronologic perspective with application to the preservation of original isotopic compositions (ages), and the possibility of dating near surface processes on Mars.

2. Experimental determination of argon diffusion in jarosite

Jarosite sample NMNH C7137, acquired from the Natural History Museum of the Smithsonian Institute was used in this study. Beyond the results presented here, the only information available for the sample is a

* Corresponding author.
E-mail address: jkula@syr.edu (J. Kula).

0012-821X/$ – see front matter © 2011 Elsevier B.V. All rights reserved.
doi:10.1016/j.epsl.2011.08.006

collection location in the Santa Eulalia District, Chihuahua, Mexico. From visual inspection and electron microprobe analysis, this sample is a coarsely crystalline, homogeneous K-jarosite (Supplementary Table 1, Supplementary Fig. 1). Details of the chemical analyses for sample characterization and $^{40}Ar/^{39}Ar$ irradiation and analytical procedures are provided in the supplementary Materials and methods.

Jarosite has been shown to break down during vacuum heating into hematite and yavapaiite at 302 °C and above (Xu et al., 2010). As it is heated, jarosite expands along the c-axis where relatively weak K–O bonds connect structural sheets of SO_4 tetrahedra and $Fe(O,OH)_6$ octahedra. The $Fe(O,OH)_6$ dehydroxylates to become FeO_6, where approximately one third of these octahedra join with SO_4 tetrahedra to form $Fe(SO_4)_2$ sheets linked together by interstitial K^+ forming nanocrystalline yavapaiite (Xu et al., 2010). The remaining FeO_6 form hematite by joining into stacks of gibbsite-type octahedral layers.

Using long-duration (4 h), low-temperature (150–285 °C), vacuum furnace step-heating with monotonically increasing temperatures, argon was incrementally extracted from three size fractions of the sample. $^{40}Ar/^{39}Ar$ age determinations are presented in Supplementary Fig. 2 and Supplementary Table 2. The heating schedule was selected to ensure the jarosite remained stable during a portion of the experiments. We infer Ar loss is via volume diffusion from stable jarosite and only gas fractions extracted at temperatures below 300 °C were used to determine diffusion kinetics (see supplementary Materials and methods). At these temperatures ^{39}Ar extracted from the three size fractions yield reproducible Arrhenius arrays (Fig. 1) with strong linearity ($r^2 \geq 0.99$), consistent with maintaining mineral stability throughout this temperature range of the step-heating experiments. Diffusion kinetics for ^{39}Ar are assumed to reflect those of $^{40}Ar^*$ (radiogenic ^{40}Ar produced by natural decay of ^{40}K). Least-squares regressions (Fig. 1) indicate an average activation energy (E) of 38.80 ± 1.58 kcal/mol and log D_o/a^2 of 6.09 ± 0.67 s^{-1} (Table 1). These values are also obtained when the three separate analyses are regressed together (Fig. 2). All results are summarized in Table 1. Because of extremely low MSWD values due to overestimated uncertainties (Wendt and Carl, 1991), omission of the first and seconds points from the regressions is based on 1) reduction in the r^2 value of the regression when included, 2) their position off of the well-defined ($r^2 \geq 0.99$) linear array (>0.5 log units) consisting of subsequent steps, and/or 3) the relatively high uncertainty associated with small signal sizes.

The Arrhenius diagram in Fig. 2 indicates that, with the exception of one point, the largest size fraction (150–200 μm) plots above the two smaller size fractions. In log D vs. 1/T space this relationship between size fractions has been interpreted as resulting from an effective diffusion radius that is between the largest crystal size analyzed and the smaller sizes with overlapping log D values (Harrison et al., 1985). However, in log D/a^2 vs. 1/T space, the larger size fraction should plot below the smaller size fractions if indeed the effective diffusion radius was smaller than the measured grain size. Fig. 2 depicts an opposite relationship between the grain sizes. However since each fraction consists of a range of crystal sizes it is unclear if an effective diffusion radius can be determined. Calculation of log D values using the maximum of each grain size range (i.e., 125, 150, 200 μm), results in a log D vs. 1/T plot with overlapping values at temperature steps 150, 200, 250, 265, and 285 °C. This may indicate that the effective diffusion radius is equal to the physical grain size and thus the apparent non-intuitive relationship between grain sizes in Fig. 2 may be caused by the mixing of a range of crystal sizes in each size fraction.

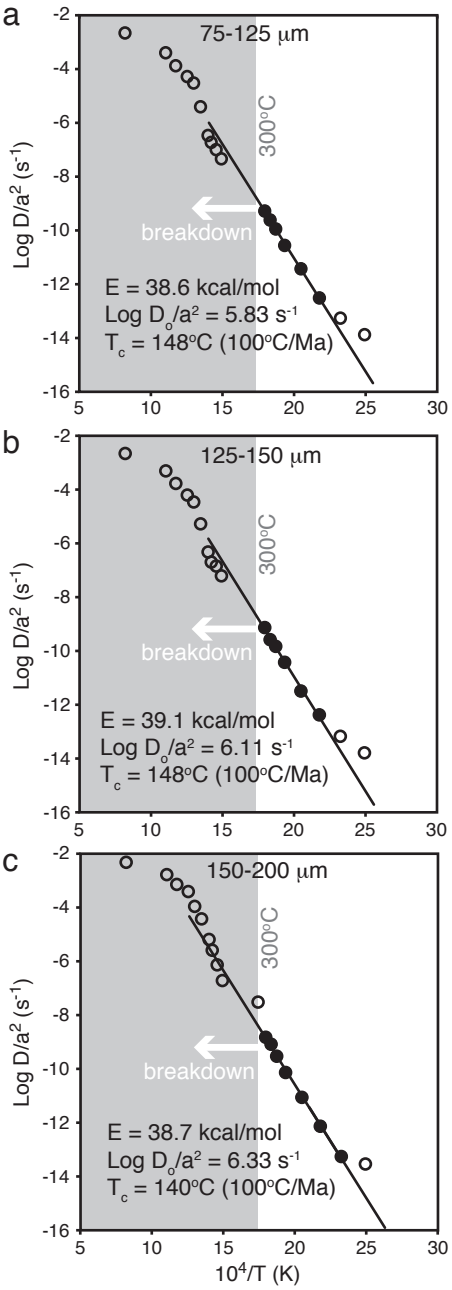

Fig. 1. Arrhenius diagrams based on incremental ^{39}Ar released during step-heat experiments. a. 75–125 μm size fraction. b. 125–150 μm size fraction. c. 150–200 μm size fraction. Least-square regression yields consistent results between grain sizes.

3. Interpreting jarosite $^{40}Ar/^{39}Ar$ ages on Earth

Based on a 100 °C/Ma cooling rate (i.e. rapid cooling at the Earth's surface), the diffusion kinetics (E, D_o/a^2) correspond to an average closure temperature (T_c) of 146 ± 30 °C (Table 1). Closure temperature refers to the temperature at the time corresponding to the measured age for a mineral (Dodson, 1973). Therefore, if these results are applicable to all jarosite, a first order, although not always correct, interpretation of $^{40}Ar/^{39}Ar$ ages is that jarosite formed below 116 °C records the timing of mineralization, and jarosite formed above 176 °C records the timing of post-formational cooling.

In supergene jarosite-forming environments on Earth such as acid mine drainage areas, acid-hypersaline lakes, and acid sulfate soils (Stoffregen et al., 2000), where mineralization occurs at surface temperatures, the measured $^{40}Ar/^{39}Ar$ age reflects the timing of jarosite formation. In cases of hypogene jarosite formation, such as thosethat occur at sulfur-rich volcanic fumaroles and hydrothermal conduits (e.g. along faults, fissures) where mineralization can occur at temperatures as high as 240 °C (e.g., Lueth et al., 2005), a jarosite $^{40}Ar/^{39}Ar$ age reflects

Table 1
Summary of diffusion parameters and fraction loss calculations.

Size fraction (μm)	E (kcal/mol)	Log D_o/a^2 (s^{-1})	Closure temperature (100 °C/Ma)	Fraction loss; 4.0 Ga	
				0 °C	22 °C
75–125 (Fig. 1a)	38.6 ± 0.6	5.83 ± 0.26	148 ± 12	0.0004	0.005
125–150 (Fig. 1b)	39.1 ± 1.3	6.11 ± 0.55	148 ± 25	0.0003	0.005
150–200 (Fig. 1c)	38.7 ± 0.7	6.33 ± 0.29	140 ± 13	0.0005	0.008
Average	38.8 ± 1.6	6.09 ± 0.67	146 ± 30	0.0004	0.006
Combined regression (Fig. 2)	37.8 ± 1.5	5.68 ± 0.63	143 ± 28	0.0006	0.008

the timing of cooling below the closure temperature, possibly marking the cessation of an episode of thermal venting.

It is noteworthy that for both supergene and hypogene environments, a measured jarosite age will constrain the timing since water was present at that location. Water is necessary for jarosite formation, although this does not mandate the occurrence of flowing or standing water at the time of mineralization (e.g., Schiffman et al., 2006). Studies of jarosite occurrence and stability indicate that a more appropriate description for a jarosite-forming environment may be a 'drying' environment rather than a 'wet' one (Fairen et al., 2009; Madden et al., 2004; Navrotsky et al., 2005). Therefore, whether fluvial, lacustrine, ground, meteoric, or vapor, a H_2O component is necessary for jarosite formation, and jarosite preservation depends largely upon the post-formational absence of water (Elwood Madden et al., 2009). Based on this understanding of jarosite formation, we infer that jarosite ages will constrain the timing of secondary mineralization related to the final waning of aqueous conditions prior to the ultimate aridification of a region.

4. Implications for determination of $^{40}Ar/^{39}Ar$ ages from Martian jarosite

The variety of processes that lead to jarosite formation on Earth result in different crystal morphologies and associated bulk mineralogy of the jarosite-bearing deposits (Alpers et al., 1992; Fernández-Remolar and Morris, 2005; Greenwood et al., 2006; Lueth et al., 2005; Schiffman et al., 2006). At present, the morphology of jarosite on Mars is unknown although hypotheses have been made based on Earth analog sites (Fairen et al., 2009). Improved constraints on Martian jarosite morphology are expected as understanding of Mars surface processes progresses with additional measurements obtained via advanced future landers and rovers. From a thermochronologic perspective, in all cases the crystal morphology of a chronometer and how it relates to the process of formation is important because 1) the conditions at the time of mineral formation need to be considered with respect to the parameters defining the chronometer's isotopic closure (especially T) to properly interpret a measured isotopic age, 2) the approximate geometry (i.e. reflecting crystal habit, K–O bond configuration) is an input parameter in the iterative calculation of bulk closure temperature (Dodson, 1973), 3) the mineral's diffusion geometry is used in the choice of the relevant fractional loss equations used to calculate Arrhenius parameters (Crank, 1975), and 4) the calculated diffusivities based on degassing experiments are typically expressed as the combined term D/a^2 where a is the diffusion length scale (e.g. crystal radius).

Although details of Martian jarosite morphology are presently unknown, the argon diffusion parameters presented here can be used along with knowledge of terrestrial jarosite to place constraints on the preservation of original isotopic signatures at the Martian surface. In addition the potential robustness of measured jarosite ages from future sample return missions can be assessed.

It is now well-demonstrated that aqueous environments have existed during early Mars history (e.g., Klingelhofer, 2004), and it is becoming increasingly convincing that aqueous environments continue to exist in the more recent Mars history (Byrne et al., 2009; Neukum et al., 2010), although more transiently. Jarosite mineral stability considerations indicate that the current Mars surface environment supports preservation of the mineral (Navrotsky et al., 2005). If the present Mars surface conditions have been maintained over the past ~4.0 Ga, (Fairén, 2010; Gaidos and Marion, 2003; Shuster and Weiss, 2005) then the Martian surface has been within the jarosite stability field for the past ~4.0 Ga.

Although mineralogically stable, residence at seemingly low temperatures ($<<T_c$) for adequately long durations can result in partial-retention zone conditions (e.g., Lister and Baldwin, 1996). The possibility of partial loss of $^{40}Ar^*$ from Martian jarosite due to long (~4.0 Ga) residence at the surface can be evaluated using the argon diffusion kinetics presented here along with constraints on Martian surface temperatures based on measurements made by the Spirit exploration rover and investigations of the ALH84001 meteorite (Cassata et al., 2010; Shuster and Weiss, 2005).

By downward extrapolation of the Arrhenius relationships (Fig. 1, Table 1) to 0° and 22 °C, an expected fractional loss can be calculated for varying residence times (Fechtig and Kalbitzer, 1966). Using the cited E and log D_o/a^2 values (Fig. 1, Table 1) these calculations predict that for jarosite residing at temperatures of 22 °C or below for 4.0 Ga, diffusive loss of less than 1% of the radiogenic ^{40}Ar will occur (Table 1). Still, the effect of seemingly small degrees of partial loss on a theoretical age spectrum can be evaluated (Lovera, 1992).

To demonstrate the likelihood that jarosite records original, undisturbed ages, model $^{40}Ar/^{39}Ar$ age spectra were produced using the AGESME program (Lovera, 1992) [see supplementary Materials and methods]. The least retentive diffusion parameters (lowest E, highest D_o/a^2 pairs as defined by uncertainties in Table 1) were used in these models to illustrate the maximum partial diffusive loss that may occur due to long-residence at low temperatures. The models are based on a single spherical domain held at 0 and 22 °C for 4.0 Ga that was 'numerically' step-heated using the 18-step heating schedule in Supplementary Table 2 with a 20-minute duration for all steps. The model results (Fig. 3) indicate that jarosite held at 0 °C for 4.0 Ga is expected to yield plateau ages within 0.4 Ma (.01%) of 4.0 Ga consisting of at least 98% of the gas release (Fig. 3a). At 22 °C, plateau ages are reduced to 95% of the gas released, but remain just within 1% (3963 Ma) of the actual 4.0 Ga age (Fig. 3b). Note again, this result is based on the least retentive E and D_o/a^2 values as constrained by the uncertainties cited in Table 1, as representing argon diffusion in jarosite, therefore it is likely to overestimate the actual partial loss at these times and temperatures.

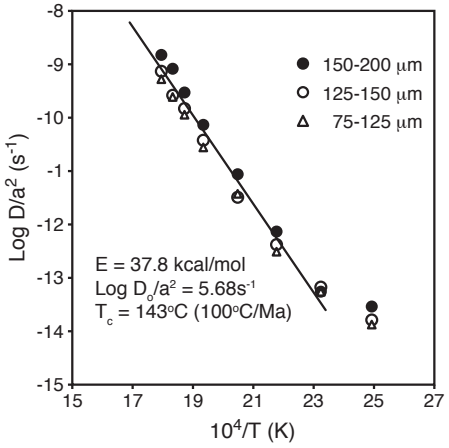

Fig. 2. Composite Arrhenius diagram from three size fractions. Only points representing ^{39}Ar released below 300 °C are included.

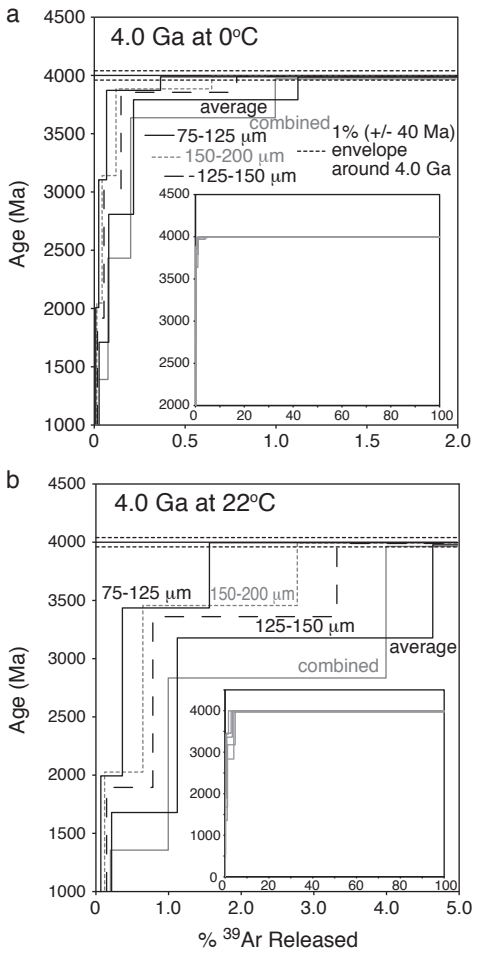

Fig. 3. Model jarosite $^{40}Ar/^{39}Ar$ age spectra for the least retentive kinetic pair (E, D_o/a^2) for each set of diffusion parameters in Table 1. a.) Model results for jarosite held at 0 °C for 4.0 Ga. Inset shows the full age spectra while the figure focuses on the initial 2.0% of the model gas release to highlight the partial loss profile. b.) Model results for jarosite held at 22 °C for 4.0 Ga. Inset shows the full age spectra while the figure focuses on the first 5.0% of the model gas release to highlight the partial loss profiles. Note both scenarios result in plateau ages within 1.0% of the 4.0 Ga crystallization age consisting of greater than 95% of the gas release.

Additionally, although loss profiles are apparent over the initial few percent of the model gas release, the majority of the age spectra yields the original crystallization age well within analytical precision and consists of far greater than 50% of the gas release (conventional minimum criteria for defining plateau ages, (e.g., McDougall and Harrison, 1999)).

A similar result to these models was presented by Landis et al. (2005) and Julian et al. (2005) where Paleoproterozoic ages (1.87 Ga) were recovered from alunite in the Tapajos gold province of Brazil. Although $^{40}Ar/^{39}Ar$ age spectra exhibited an apparent loss profile with ages progressively increasing with temperature, consistency in plateau ages (>50% of the gas release) indicates the alunite effectively preserved original ages over billion year timescales. As minerals of the same group (substituting Al^{3+} and Fe^{3+} for alunite and jarosite, respectively), the recovery of Paleoproterozoic ages in alunite may lend support to the model results presented here as a mineralogical analog for the long-term retention of argon in sulfates.

5. Implications for Mars jarosite sample return

Because 22 °C is a maximum temperature based on modeling of meteorite age spectra, and also represents the maximum temperature measured by the Spirit rover, model ages assuming this temperature persisted on Mars for 4.0 Ga reflect the maximum estimate for long-duration partial retention of argon. Therefore, the diffusion parameters presented here predict that jarosite collected from the Mars surface and transported to Earth for laboratory analysis should record the original ages of formation, likely reflecting the time since water was present at the sample locality. $^{40}Ar/^{39}Ar$ ages from jarosite samples collected along a vertical profile, such as that investigated by the Opportunity MER (Grotzinger et al., 2005), may record the timing of downward migration of an aridification front during water table retreat. This is dependent on the duration of the retreat. Additionally, jarosite is not a very robust mineral like zircon (e.g., http://www.geology.wisc.edu/zircon/zircon_home.html) but rather quite friable. It readily breaks down into hematite and yavapaiite at relatively low temperatures (beginning at 300 °C, and completely by 350 °C (Xu et al., 2010)), is susceptible to rapid dissolution in water (Elwood Madden et al., 2009), and it is precipitated and destroyed by erosion/dissolution on very short timescales in some settings (Schiffman et al., 2006). Based on its susceptibility to breakdown, preservation of jarosite on Mars requires that it has not experienced a significant thermal event (i.e. volcanism, impact) that would result in age compromising diffusive loss of argon as the mineral would not survive.

The Mars surface is dominated by basaltic compositions in the form of lavas and reworked sediments and ash, affording an abundant supply of Fe and S available to interact with the evaporating/sublimating surface and groundwaters/ice. The recent discovery of jarosite in the Mawrth Vallis region (Farrand et al., 2009) supports the premise that on Mars, jarosite is highly likely to form anywhere water existed, especially during the waning stages of drying aqueous environments (e.g., Mccubbin et al., 2009). Therefore, a distribution of Martian jarosite ages could reflect locations where past aqueous environments once persisted and importantly, have not since been affected by astrobiologically catastrophic events such as impacts and volcanism, thus marking sites possibly favorable for biological development.

Supplementary materials related to this article can be found online at doi:10.1016/j.epsl.2011.08.006.

Acknowledgments

This study was supported by the New York Center for Astrobiology and the NASA Astrobiology Institute (grant NNA09DA80A). Jarosite samples were provided by the Department of Mineral Sciences, Smithsonian Institute thanks to the efforts of Cathleen Brown and Bruce Watson. Jon Price assisted with the EMPA chemical analyses. We appreciate comments and suggestions provided by Virgil Lueth and an anonymous reviewer.

References

Alpers, C.N., Rye, R.O., Nordstrom, D.K., White, L.D., King, B.-S., 1992. Chemical crystallographic and stable isotopic properties of alunite and jarosite from acid-hypersaline Australian lakes. Chem. Geol. 96, 203–226.
Aubrey, A., Cleaves, H.J., Chalmers, J.H., Skelley, A.M., Mathies, R.A., Grunthaner, F.J., Ehrenfreund, P., Bada, J.L., 2006. Sulfate minerals and organic compounds on Mars. Geology 34, 357.
Burger, P.V., Papike, J.J., Shearer, C.K., Karner, J.M., 2009. Jarosite growth zoning as a recorder of fluid evolution. Geochim. Cosmochim. Acta 73, 3248–3259.
Byrne, S., Dundas, C.M., Kennedy, M.R., Mellon, M.T., Mcewen, A.S., Cull, S.C., Daubar, I.J., Shean, D.E., Seelos, K.D., Murchie, S.L., Cantor, B.A., Arvidson, R.E., Edgett, K.S., Reufer, A., Thomas, N., Harrison, T.N., Posiolova, L.V., Seelos, F.P., 2009. Distribution of mid-latitude ground ice on Mars from new impact craters. Science 325, 1674–1676.
Cassata, W., Shuster, D., Renne, P.R., Weiss, B.P., 2010. Evidence for shock heating and constraints on Martian surface temperatures revealed by $^{40}Ar/^{39}Ar$ thermochronometry of Martian meteorites. Geochim. Cosmochim. Acta 74, 6900–6920.
Christensen, P., Bandfield, J., Clark, R., Edgett, K., Hamilton, V., Hoefen, T., Kieffer, H., Kuzmin, R., Lane, M., Malin, M., 2000. Detection of crystalline hematite mineralization on Mars by the Thermal Emission Spectrometer — evidence for near-surface water. J. Geophys. Res. 105, 9623–9642.
Crank, J., 1975. The Mathematics of Diffusion, 2nd edition. Oxford University Press, NY.
Dodson, M., 1973. Closure temperature in cooling geochronological and petrological systems. Contrib. Mineral. Petrol. 40, 259–274.

Elwood Madden, M.E., Madden, A.S., Rimstidt, J.D., 2009. How long was Meridiani Planum wet? Applying a jarosite stopwatch to determine the duration of aqueous diagenesis. Geology 37, 635–638.
Fairén, A.G., 2010. A cold and wet Mars. Icarus 208, 165–175.
Fairen, A.G., Schulze-Makuch, D., Rodriguez, A.P., Fink, W., Davila, A.F., Uceda, E.R., Furfaro, R., Amils, R., McKay, C.P., 2009. Evidence for Amazonian acidic liquid water on Mars—a reinterpretation of MER mission results. Planet. Space Sci. 57, 276–287.
Farrand, W.H., Glotch, T.D., Rice, J.W., Hurowitz, J.A., Swayze, G.A., 2009. Discovery of jarosite within the Mawrth Vallis region of Mars: implications for the geologic history of the region. Icarus 1–11.
Fechtig, H., Kalbitzer, S., 1966. The diffusion of argon in potassium-bearing solids. In: Schaeffer, O., Zahringer, J. (Eds.), Potassium–Argon Dating. Springer Verlag, pp. 68–106.
Fernández-Remolar, D., Morris, R., 2005. The Río Tinto Basin, Spain: mineralogy, sedimentary geobiology, and implications for interpretation of outcrop rocks at Meridiani Planum, Mars. Earth Planet. Sci. Lett. 240, 149–167.
Gaidos, E., Marion, G., 2003. Geological and geochemical legacy of a cold early Mars. J. Geophys. Res. 108, 5055.
Greenwood, J., Gilmore, M., Blake, R., 2006. Nascent jarosite mineralization of Sulphur Springs, St. Lucia, WI: implications for Meridiani jarosite formation. 37th Annual Lunar and Planetary Science Conference.
Grotzinger, J., Arvidson, R., Bell, J., 2005. Stratigraphy and sedimentology of a dry to wet eolian depositional system, burns formation, Meridiani Planum, Mars. Earth Planet. Sci. Lett. 240, 11–72.
Harrison, T.M., Duncan, I., McDougall, I., 1985. Diffusion of ^{40}Ar in biotite: temperature, pressure and compositional effects. Geochim. Cosmochim. Acta 49, 2461–2468.
http://www.geology.wisc.edu/zircon/zircon_home.html, Zircons are Forever. University of Wisconsin-Madison.
Klingelhofer, G., 2004. Jarosite and hematite at Meridiani Planum from opportunity's Mossbauer spectrometer. Science 306, 1740–1745.
Kotler, J., Hinman, N., Yan, B., Stoner, D., Scott, J., 2008. Glycine identification in natural jarosites using laser desorption Fourier transform mass spectrometry: implications for the search for life on Mars. Astrobiology 8, 253–266.
Landis, G.P., Snee, L.W., Juliani, C., 2005. Evaluation of argon ages and integrity of fluid-inclusion compositions: stepwise noble gas heating experiments on 1.87 Ga alunite from Tapajos Province, Brazil. Chem. Geol. 215, 127–153.
Lister, G., Baldwin, S., 1996. Modelling the effect of arbitrary PTt histories on argon diffusion in minerals using the MacArgon program for the Apple Macintosh. Tectonophysics 253, 83–109.
Lovera, O.M., 1992. Computer programs to model ^{40}Ar/^{39}Ar diffusion data from multidomain samples. Comput. Geosci. 18, 789–813.
Lueth, V., Rye, R., Peters, L., 2005. "Sour gas" hydrothermal jarosite: ancient to modern acid-sulfate mineralization in the southern Rio Grande Rift. Chem. Geol. 215, 339–360.
Julian, C., Rye, R.O., Nunes, C.M.D., Snee, L.W., Correa Silva, R.H., Monteiro, L.V.S., Bettencourt, J.S., Neumann, R., Neto, A.A., 2005. Paleoproterooic high-sulfidation mineralization in the Tapajos gold province, Amazonian Craton, Brazil: geology, mineralogy, alunite argon age, and stable-isotope constraints. Chem. Geol. 215, 95–125.
Madden, M., Bodnar, R., Rimstidt, J., 2004. Jarosite as an indicator of water-limited chemical weathering on Mars. Nature 431, 821–823.
Mccubbin, F.M., Tosca, N.J., Smirnov, A., Nekvasil, H., Steele, A., Fries, M., Lindsley, D.H., 2009. Hydrothermal jarosite and hematite in a pyroxene-hosted melt inclusion in Martian meteorite Miller Range (MIL) 03346: implications for magmatic-hydrothermal fluids on Mars. Geochim. Cosmochim. Acta 73, 4907–4917.
McDougall, I., Harrison, T.M., 1999. Geochronology and Thermochronology by the ^{40}Ar/^{39}Ar Method, 2nd edition. Oxford University Press, New York.
Navrotsky, A., Forray, F., Drouet, C., 2005. Jarosite stability on Mars. Icarus 176, 250–253.
Neukum, G., Basilevsky, A., Kneissl, T., Chapman, M., van Gasselt, S., Michael, G., Jaumann, R., Hoffmann, H., Lanz, J., 2010. The geologic evolution of Mars: episodicity of resurfacing events and ages from cratering analysis of image data and correlation with radiometric ages of Martian meteorites. Earth Planet. Sci. Lett. 294, 204–222.
Papike, J., Karner, J., Shearer, C., 2006. Comparative planetary mineralogy: implications of Martian and terrestrial jarosite. A crystal chemical perspective. Geochim. Cosmochim. Acta 70, 1309–1321.
Schiffman, P., Zierenberg, R., Marks, N., Bishop, J., Dyar, M., 2006. Acid-fog deposition at Kilauea volcano: a possible mechanism for the formation of siliceous-sulfate rock coatings on Mars. Geology 34, 921–924.
Shuster, D.L., Weiss, B.P., 2005. Martian surface paleotemperatures from thermochronology of meteorites. Science 309, 594–597.
Squyres, S., Knoll, A., 2005. Sedimentary rocks at Meridiani Planum: origin, diagenesis, and implications for life on Mars. Earth Planet. Sci. Lett. 240, 1–10.
Stoffregen, R.E., Alpers, C.N., Jambor, J.L., 2000. Alunite–jarosite crystallography, thermodynamics, and geochronology. In: Alpers, C.N., et al. (Ed.), Sulfate Minerals — Crystallography, Geochemistry and Environmental Significance: Reviews in Mineralogy and Geochemistry, pp. 453–479.
Vasconcelos, P., Brimhall, G., Becker, T., Renne, P., 1994. ^{40}Ar/^{39}Ar analysis of supergene jarosite and alunite: implications to the paleoweathering history of the western USA and West Africa. Geochim. Cosmochim. Acta 58, 401–420.
Wendt, I., Carl, C., 1991. The statistical distribution of the mean squared weighted deviation. Chem. Geol. 86, 275–285.
Xu, H., Zhao, Y., Vogel, S., Hickmott, D., Daemen, L., Hartl, M., 2010. Thermal expansion and decomposition of jarosite: a high-temperature neutron diffraction study. Phys. Chem. Miner. 37, 73–82.